Eur. Phys. J. C (2008) 57: 515–523
DOI 10.1140/epjc/s10052-008-0750-z

THE EUROPEAN PHYSICAL JOURNAL C

Regular Article - Experimental Physics

Lee-Yang circle analysis of e^+e^- and $p\overline{p}$ generalized multiplicity distribution

A. Dewanto[1,a], **A.H. Chan**[1], **C.H. Oh**[1], **R. Chen**[2], **K. Sitaram**[2]

[1]Department of Physics, National University of Singapore, 2 Science Drive 3, Singapore 117542, Singapore
[2]Raffles Junior College, 10 Bishan Street 21, Singapore 574013, Singapore

Received: 7 July 2008 / Revised: 1 September 2008 / Published online: 24 September 2008

Abstract We study the evolution of Lee-Yang zeros structure of generalized multiplicity distribution (GMD) in high energy collision. Starting our study with electron-positron e^+e^- scattering data, we extend the study by Chan and Chew (Z. Phys. C 55:503, 1992) on TASSO and AMY multiplicity data for $\sqrt{s} = 14$, 22, 34.8, 43.6 and 57 GeV to the ones from DELPHI and OPAL Collaboration for $\sqrt{s} = 91$, 133, 161, 172, 183 and 189 GeV. We compare the results with the Lee-Yang structure for proton-antiproton $p\overline{p}$ at $\sqrt{s} = 200$, 546 and 900 GeV from UA5 Collaboration. Our preliminary result shows that there is indeed a change in the shape and size of the Lee-Yang zeros with increasing energy, accompanied by the development of the so-called "ear"-like structure in the Lee-Yang plot. We expect that the development of this "ear"-like structure is related to the "shoulder" structure in the multiplicity data, which further indicates an ongoing phase transition from soft to semihard scattering. We also extend our prediction to LHC's $\sqrt{s} = 14$ TeV. Insert your abstract here.

Keywords Multiplicity distribution · Lee-Yang zeros

1 Introduction

In anticipation for the upcoming operation of LHC in 2008, multiparticle production has again become one of major discussion in high energy physics recently [1, 2]. In the previous studies, negative binomial distribution (NBD), which Giovannini has shown as a solution to the stochastic branching equation [3] that governs the dynamics of multiparticle production, is usually used to describe the experimental data. Superposition of 2 NBDs was further studied by Giovannini et al. to explain the "shoulder"-like structure that starts to appear at $\sqrt{s}$ as low as 91 GeV [4], and becomes more pronounced as energy increases [5, 6].

However, NBD is not the only solution to the stochastic branching equation that governs the evolution of multiparticle production. Chew et al. introduced generalized multiplicity distribution (GMD) as an alternative solution to study $p\overline{p}$ and pp multiplicity distributions [7]. It was noted by Wroblewski [8] that GMD also gives an excellent fit for e^+e^- data and a reasonably good fit to $p\overline{p}$ and pp data. The former was first studied in detail by Chan and Chew [9] up to 57 GeV using data from TASSO and AMY Collaboration. In this letter, we would like to extend the study to the full phase space multiplicity distributions data from DELPHI's $\sqrt{s} = 91$ GeV, OPAL's $\sqrt{s} = 133$, 161, 172, 183 and 189 GeV, and to UA5's $\sqrt{s} = 200$, 546 and 900 GeV for $p\overline{p}$ case. We are also interested to study how the Lee-Yang circles will evolve as the scattering energy increases from 14 GeV all the way to 900 GeV.

Hence, we would like to by reminding the reader on how GMD is derived, followed by the analysis of e^+e^- and $p\overline{p}$ full phase space multiplicity data in the results and discussions and comparative study between the two.

2 Formalism and derivation of generalized multiplicity distribution

Giovannini showed that the total multiplicity distribution of partons inside a jet calculus can be written in the following equation [3]

$$\frac{dP_{n,m}}{dt} = -(An + \tilde{A}m + Bn)P_{n.m} + A(n-1)P_{n-1,m} + \tilde{A}mP_{n-1,m} + B(n+1)P_{n+1,m-2} \quad (1)$$

[a] e-mail: phyda@nus.edu.sg

also known as the stochastic branching equation, where

$$t = \frac{6}{11N_c - 2N_f} \ln\left[\frac{\ln(Q^2/\mu^2)}{\ln(Q_0^2/\mu^2)}\right] \tag{2}$$

is the QCD evolution parameter, with Q is the initial parton invariant mass, Q_0 is the hadronization mass, μ is a QCD mass scale (in GeV), $N_c = 3$ (number of colors), and $N_f = 4$ (number of flavors). $P_{n,m}$ is the probability distribution of n gluons and m quarks at QCD evolution, with A, $\tilde{A}$ and B refer to the average probabilities of the branching process $g \to gg$, $q \to qg$, and $g \to q\overline{q}$ respectively.

For fixed m and number of n gluons at t, we can rewrite (1) to

$$\frac{dP_n}{dt} = -(An + \tilde{A}m + Bn)P_n + A(n-1)P_{n-1} + \tilde{A}mP_{n-1} + B(n+1)P_{n+1} \tag{3}$$

where GMD is the solution of it. To solve (3) analytically, denote a probability generating function to be

$$f(t,s) = \sum_{n=0}^{\infty} P_n s^n. \tag{4}$$

Capella et al. shows that (4) has similarity to grand canonical partition function in statistical physics [10]. In particular, by truncating (4) and set it to zero, one can always find a set of complex solutions which, upon plotting, will form a circle in the complex plane as studied by Lee and Yang [11, 12]. This has further been studied by Brooks et al. [13] and Brambilla et al. [14] for the case of Poisson distribution and NBD.

Next we consider

$$\frac{\partial f}{\partial t} = \sum_{n=0}^{\infty} \frac{dP_n}{dt} s^n. \tag{5}$$

It can be shown that

$$\frac{\partial f}{\partial t} = (1-s)(B - As)\frac{\partial f}{\partial s} - \tilde{A}m(1-s)f. \tag{6}$$

To solve this first order partial differential equation, we introduce the subsidiary equation

$$dt = \frac{ds}{(1-s)(As-B)} = -\frac{df}{\tilde{A}m(1-s)f}. \tag{7}$$

Thus, solving the first and second term in (7) will result in

$$e^{t(A-B)}\left(\frac{1-s}{As-B}\right) = \text{constant} \tag{8}$$

while solving the second and third term in (7) will give

$$\frac{\tilde{A}}{A}m\ln(As-B) + \ln f = \text{constant}. \tag{9}$$

Thus we can write the following relationship in term of a function Ψ

$$\frac{\tilde{A}}{A}m\ln(As-B) + \ln f = \Psi\left[e^{t(A-B)}\left(\frac{1-s}{As-B}\right)\right]. \tag{10}$$

Setting the initial condition to $f(t=0,s) = s^{k'}$ (hence k' is the initial number of gluons in average sense), one obtains

$$f = \left[A\left(\frac{1+XB}{1+XA}\right) - B\right]^{\frac{m\tilde{A}}{A}} [As-B]^{-\frac{m\tilde{A}}{A}} \times \left[\frac{1+XB}{1+XA}\right]^{k'} \tag{11}$$

where $X = e^{t(A-B)}(\frac{1-s}{As-B})$. At this stage, we neglect B as in [9] (i.e. $B = 0$) so that (11) will reduce to the generating function of GMD

$$f = [s + (1-s)e^{At}]^{-k}\left[1 + \frac{1-s}{s}e^{At}\right]^{-k'} \tag{12}$$

where $k = \frac{m\tilde{A}}{A}$ is related to the initial number of quarks in average sense.

Finally, using $P_n = \frac{1}{n!}\frac{\partial^n f}{\partial s^n}|_{s=0}$, we get the solution to (3), namely the generalized multiplicity distribution (GMD) for $B = 0$ [7]

$$P_{\text{GMD}}(n) = \frac{(n+k-1)!}{(n-k')!(k'+k-1)!} \times \left(\frac{\overline{n}-k'}{\overline{n}+k}\right)^{n-k'}\left(\frac{k+k'}{\overline{n}+k}\right)^{k+k'} \tag{13}$$

where $\overline{n} = (k'+k)e^{At} - k$ and $n > k'$. GMD reduces to negative binomial distribution (NBD) when $k' = 0$, and it also reduces to Furry-Yule distribution (FYD) proposed by Hwa and Lam [15] when $k = 0$.

To compute the q-th moments C_q we use the following

$$C_q = \frac{\overline{n^q}}{\overline{n}^q} \tag{14}$$

where from (12) we have $\frac{\partial f}{\partial s}|_{s=1} = \overline{n}$, and we can compute $\overline{n^q}$ in the following way [9]

$$\begin{aligned}
\overline{n^2} &= \left.\frac{\partial^2 f}{\partial s^2}\right|_{s=1} + \left.\frac{\partial f}{\partial s}\right|_{s=1}, \\
\overline{n^3} &= \left.\frac{\partial^3 f}{\partial s^3}\right|_{s=1} + 3\left.\frac{\partial^2 f}{\partial s^2}\right|_{s=1} + \left.\frac{\partial f}{\partial s}\right|_{s=1}, \\
\overline{n^4} &= \left.\frac{\partial^4 f}{\partial s^4}\right|_{s=1} + 6\left.\frac{\partial^3 f}{\partial s^3}\right|_{s=1} + 7\left.\frac{\partial^2 f}{\partial s^2}\right|_{s=1} + \left.\frac{\partial f}{\partial s}\right|_{s=1},
\end{aligned} \tag{15}$$

$$\overline{n^5} = \frac{\partial^5 f}{\partial s^5}\bigg|_{s=1} + 10\frac{\partial^4 f}{\partial s^4}\bigg|_{s=1} + 25\frac{\partial^3 f}{\partial s^3}\bigg|_{s=1} + 15\frac{\partial^2 f}{\partial s^2}\bigg|_{s=1} + \frac{\partial f}{\partial s}\bigg|_{s=1}.$$

However, since the data points are truncated at certain $n = M$, we compute the cumulants using $\overline{n^q} = \sum_{n=0}^{M} n^q P_n$, whose result will converge with those given in (15) at $n \to \infty$.

3 Results and discussions

In the previous study, Chan and Chew [9] have examined the full phase space multiplicity distribution of e^+e^- data for $\sqrt{s}$ ranging from 14 to 43.6 GeV (TASSO Collaboration) [16], and that for 57 GeV (AMY Collaboration) [17], which we summarize in Table 1.

In our work here, we extend the study to the e^+e^- full phase space data from DELPHI for $\sqrt{s} = 91$ GeV [18], and those from OPAL Collaboration for $\sqrt{s} = 133$, 161, 172, 184 and 189 GeV [19–21]. In addition, we also analyze the Lee-Yang solutions from the generating functions in (4) of the scattering energies using our GMD probability distribution.

We perform the chi-square test of GMD using the experimental data taken from DELPHI and OPAL Collaboration for respective $\sqrt{s}$ to determine the best-fit value of k and k' and use the set of equations in (15) to compute the moments. The result is tabulated in Table 2. Except for $\sqrt{s} = 91$ GeV data produced by DELPHI Collaboration, the χ^2-fit for the OPAL Collaboration data is less than 1. In fact, comparing the two tables, the χ^2-fit of OPAL data is generally better than the χ^2-fit of TASSO and AMY data.

Having checked that GMD gives an excellent description for a wide range of e^+e^- data ranging from 14 to 189 GeV, we continue our analysis with plotting the Lee-Yang zeros of the above-mentioned data. The plots are shown in Fig. 1 and Fig. 2. We notice that, as the scattering energy increases, the Lee-Yang plots are becoming more rounded. At the same time, the size of the plots is also converging to unity (Fig. 2). We also notice that there are few points in the Lee-Yang plot of $\sqrt{s} = 91$ GeV and above, which do not seem to fit to the trend of the curve. However, we suspect that the appearance of those points are due to high error bars of the first few data in the scattering experiment. After all, we can always smoothen the plot by starting the polynomials at higher terms ($n = 12, 14, \ldots$). For example, by discarding the first few data whose error exceeds 50% of the observed data, we can smoothen the Lee-Yang plot as shown in Fig. 3.

At this point, we would also like to bring into attention the difference between our result and an earlier study conducted by Brooks et al. [13] and Giovannini et al. [14], namely that GMD's Lee-Yang zeros exhibit both left-right symmetry as well as top-bottom symmetry. This feature distinguishes the zeros from GMD and those from NBD, as NBD's Lee-yang circle exhibits only top-bottom symmetry, i.e. it was closed on the left and open on the right. This suggests that the feature of GMD's Lee-Yang zeros can essentially be simplified to a quarter of the circle in the complex plane. Hence, carrying out the analysis of the zeros at a particular quadrant of the complex plane is as good as carrying the analysis in its entirety, which may come as something convenient when computation resource is limited. Furthermore, this feature may seem unique to GMD's Lee-Yang structure only, and it is independent of scattering energy or collision type (i.e. it persists at $p\overline{p}$ collision as we will see soon).

Table 1 GMD parameters in (13) for TASSO and AMY data, taken from [9]. The numbers inside the parentheses refer to the total number of multiplicity data N

$\sqrt{s}$ (GeV)	$\overline{n}$	k	k'	C_2	C_3	C_4	C_5	χ^2/N
14	9.30	38.00	1.65	1.11	1.33	1.73	2.41	1.10 (13)
22	11.30	32.00	1.58	1.10	1.31	1.67	2.28	0.27 (14)
34.8	13.59	25.00	1.80	1.09	1.29	1.63	2.20	1.03 (18)
43.6	15.08	21.00	2.00	1.09	1.28	1.62	2.17	0.80 (19)
57	17.19	25.00	2.00	1.08	1.25	1.54	2.02	0.66 (20)

Table 2 GMD parameters in (13) for DELPHI and OPAL data

$\sqrt{s}$ (GeV)	$\overline{n}$	k	k'	C_2	C_3	C_4	C_5	χ^2/N
91	21.20	15.57	2.00	1.089	1.281	1.615	2.169	1.234 (25)
133	23.61	12.15	2.00	1.062	1.194	1.416	1.766	0.238 (25)
161	24.45	12.26	2.00	1.095	1.301	1.663	2.270	0.090 (25)
172	25.54	14.96	2.00	1.086	1.270	1.589	2.117	0.062 (28)
183	26.85	13.35	2.00	1.088	1.280	1.614	2.168	0.545 (28)
189	26.94	11.86	2.00	1.095	1.301	1.662	2.269	0.186 (28)

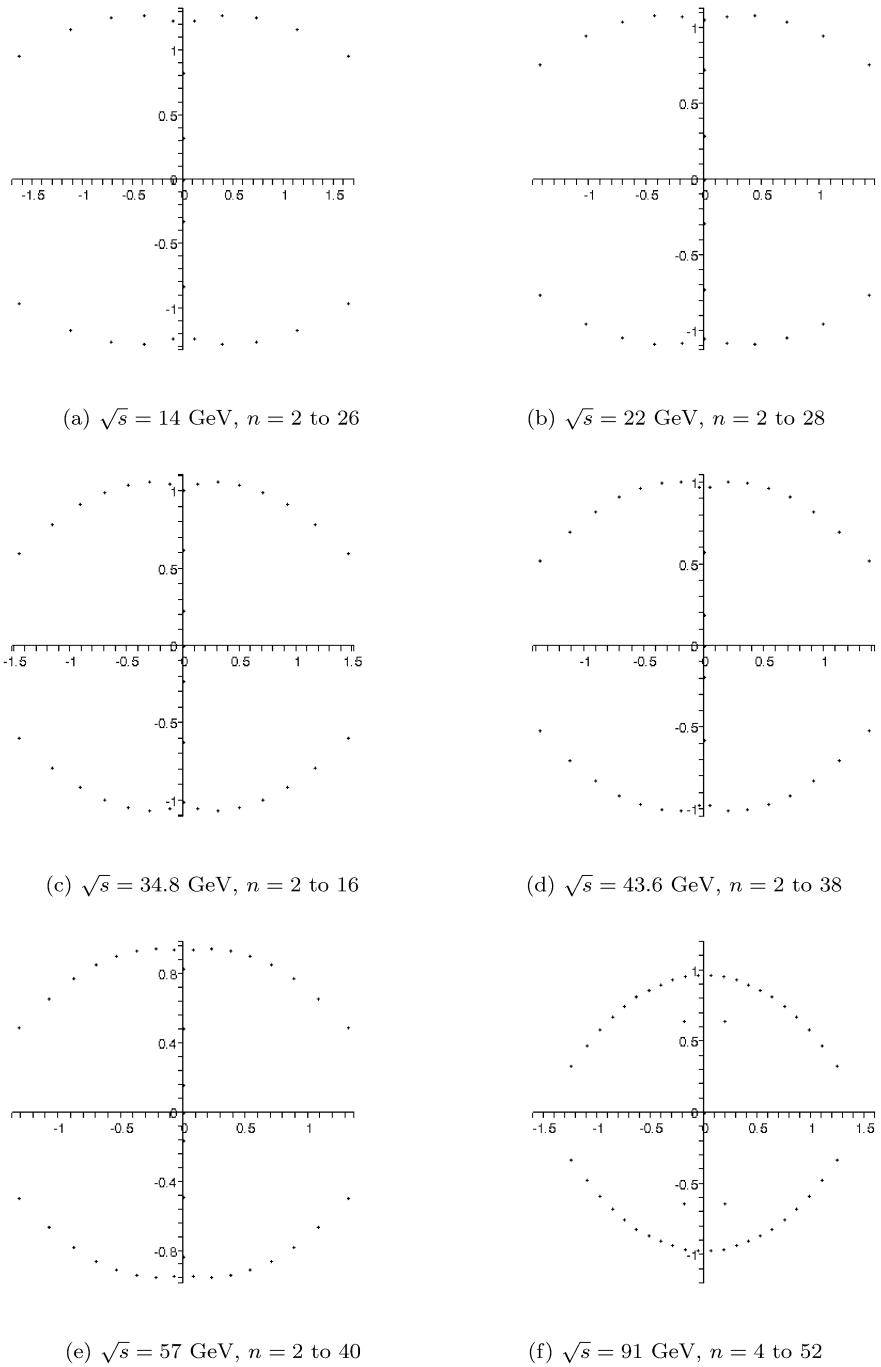

(a) $\sqrt{s} = 14$ GeV, $n = 2$ to 26

(b) $\sqrt{s} = 22$ GeV, $n = 2$ to 28

(c) $\sqrt{s} = 34.8$ GeV, $n = 2$ to 16

(d) $\sqrt{s} = 43.6$ GeV, $n = 2$ to 38

(e) $\sqrt{s} = 57$ GeV, $n = 2$ to 40

(f) $\sqrt{s} = 91$ GeV, $n = 4$ to 52

Fig. 1 GMD Lee-Yang zeros plot ($\sum_{n=0}^{M} P_n z^n = 0$) for $\sqrt{s} = 14$ to 91 GeV

We, however, notice right away that the e^+e^- multiplicity distributions show some characteristics that distinguish them from their $p\overline{p}$ and pp counterparts, which we have studied earlier in [22] using the multiplicity data from UA5 Collaboration at $\sqrt{s} = 200, 546$ and 900 GeV [23, 24]. Here, we have to take into account the "shoulder"-like structure at the tail of the distribution that has become too significant to neglect. To explain the "shoulder"-like structure in $p\overline{p}$ multiplicity distribution plots, Giovannini suggested that a multiplicity dynamics is actually a result from superposition of two events, the soft (without minijet) and semihard (with minijets) scattering events [25]. As the scattering energy goes higher, the semihard component becomes more significant. Thus, the distribution function P_n should also be written as the superposition of 2 GMDs, one for soft and the other for semihard term respectively

$$P_n = \alpha_{\text{soft}} P_{\text{GMD}}(\overline{n}_{\text{soft}}, k_{\text{soft}}, k'_{\text{soft}}) + (1 - \alpha_{\text{soft}}) P_{\text{GMD}} \times (\overline{n}_{\text{semihard}}, k_{\text{semihard}}, k'_{\text{semihard}}). \quad (16)$$

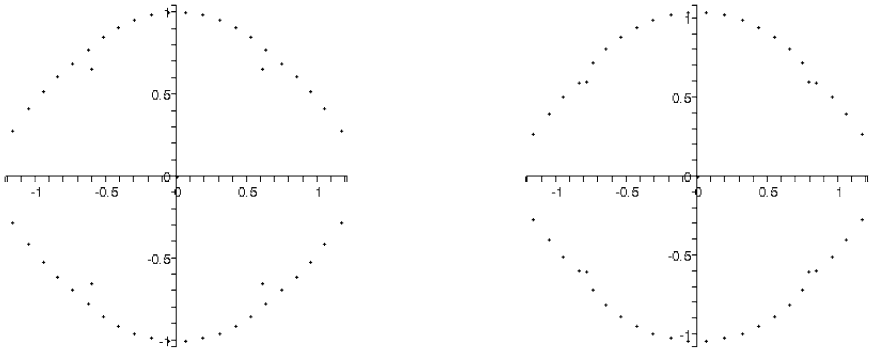

(a) $\sqrt{s} = 133$ GeV, $n = 6$ to 54

(b) $\sqrt{s} = 161$ GeV, $n = 8$ to 56

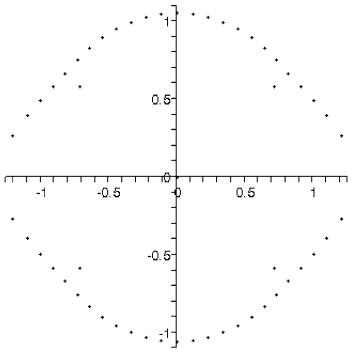

(c) $\sqrt{s} = 172$ GeV, $n = 8$ to 62

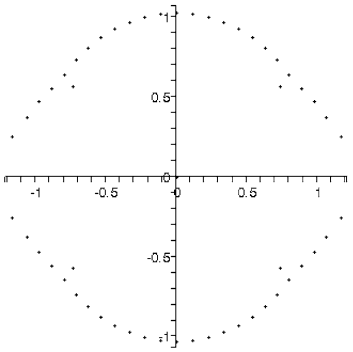

(d) $\sqrt{s} = 183$ GeV, $n = 8$ to 62

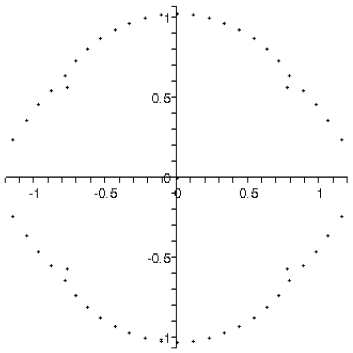

(e) $\sqrt{s} = 189$ GeV, $n = 8$ to 62

Fig. 2 GMD Lee-Yang zeros plot ($\sum_{n=0}^{M} P_n z^n = 0$) for $\sqrt{s} = 133$ to 189 GeV

We quote the parameters we used in [22] below (see Table 3), while the Lee-Yang plots are shown in Fig. 4.

Comparing $p\overline{p}$ Lee-Yang plots with those of e^+e^-, we can observe a progressive formation of the so-called "ear" structure in the plots, i.e. the tail of zeros from the upper-half and the lower-half of the plots. $p\overline{p}$ Lee-Yang zeros are forming an almost perfect unit circle, while at the same time the "ear" in $p\overline{p}$ Lee-Yang plots is converging to real axis.

Lee and Yang suggested that when the zeros converge, it is an indication of an ongoing phase transition, in which the transition occurs at the point of convergence [11]. Hence, we try to understand the converging Lee-Yang zeros in UA5 data as a hint at a transition from soft to semihard scattering. Such transition, however, is not noticed in the e^+e^- Lee-Yang plots at $\sqrt{s} < 133$ GeV, as no convergence point is yet noticed, indicating that the soft events mostly, if not purely, dominate at this energy range.

In relation to our original interpretation of k and k' in GMD (which refer to the number of quarks and gluons respectively), we noted that as $\sqrt{s}$ increases, k decreases while

Fig. 3 GMD Lee-Yang zeros plot ($\sum_{n=0}^{M} P_n z^n = 0$) for $\sqrt{s} = 133$ to 189 GeV, in which first few data whose error bar too large, is ignored

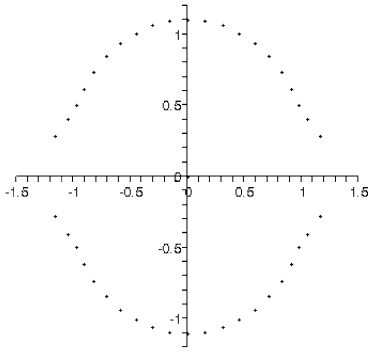

(a) $\sqrt{s} = 133$ GeV, $n = 12$ to 54

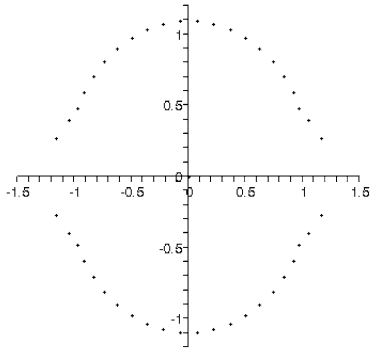

(b) $\sqrt{s} = 161$ GeV, $n = 12$ to 56

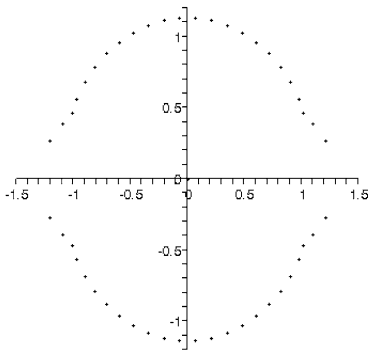

(c) $\sqrt{s} = 172$ GeV, $n = 14$ to 62

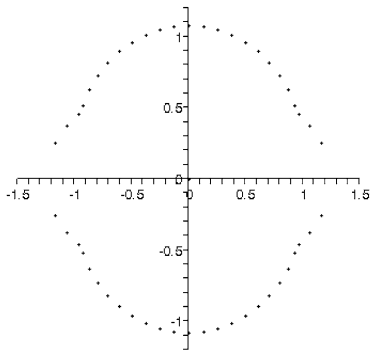

(d) $\sqrt{s} = 183$ GeV, $n = 12$ to 62

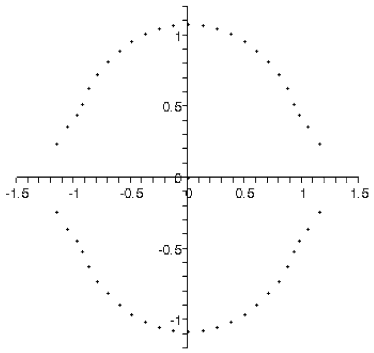

(e) $\sqrt{s} = 189$ GeV, $n = 12$ to 62 on the right

Table 3 GMD parameters in (16) for UA5 data

$\sqrt{s}$ (GeV)	α	$\overline{n}_{\text{soft}}$	$\overline{n}_{\text{semihard}}$	k_{soft}	k'_{soft}	k_{semihard}	k'_{semihard}	χ^2/N
200	0.901	19.47	41.74	2.16	2.00	2.16	4.00	0.61(37)
546	0.796	24.21	52.39	1.45	2.00	1.45	8.00	5.35(57)
900	0.740	26.57	57.76	1.25	2.00	1.25	12.00	2.97(63)
14000	0.431	39.52	88.16	0.70	2.00	0.70		

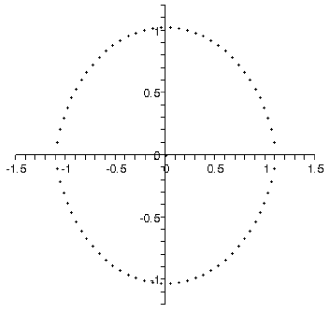

(a) $\sqrt{s} = 200$ GeV, $k'_{semihard} = 4$, $n = 4$ to 76

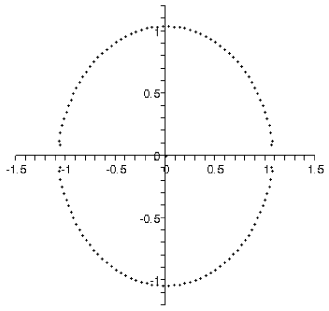

(b) $\sqrt{s} = 546$ GeV, $k'_{semihard} = 8$, $n = 8$ to 120

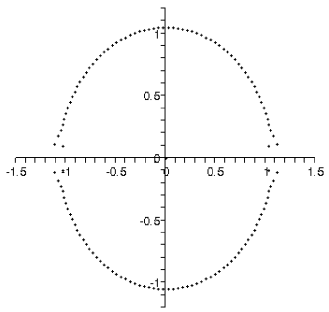

(c) $\sqrt{s} = 900$ GeV, $k'_{semihard} = 12$, $n = 12$ to 136

Fig. 4 GMD Lee-Yang zeros plot ($\sum_{n=0}^{M} P_n z^n = 0$) for $\sqrt{s} = 200$ to 900 GeV

k' increases. This implies that as the scattering energy increases, the scattering is becoming less dominated by the quarks, while the gluons are becoming more dominant. Due to the constraint $k' < n$ in GMD probability function of (13), k' is saturated at 2.00, while k has dropped significantly. However, the fact that k is still higher than k' indicates that scattering events are dominated by quarks at LEP energy range.

While k_{soft} is still saturated at 2.00, we can afford to have $k'_{\text{semihard}} > 2.00$ as to ensure that the semihard component is significant enough for P_n to describe the experimental data. However, as k'_{semihard} increases, k_{semihard} and k_{soft} have dropped to less than 1 at $\sqrt{s} = 14$ TeV (see Table 3). The fact that k'_{soft} and k'_{semihard} are higher than k_{soft} and k_{semihard} indicates that scattering events are dominated by gluons at SPS and higher energy range, as opposite to LEP cases.

Similar pattern is also noticed in our computational work at $\sqrt{s} = 14$ TeV (see Fig. 5). In our study, we vary the numerical value of k'_{semihard}, while keeping the other parameters constant. It is clear from our study that increasing the numerical value of k'_{semihard} will cause the "shoulder" structure in the multiplicity data as well as the "ear" structure in the Lee-Yang plots to be more pronounced. This again leads us to our conclusion that at $\sqrt{s} = 14$ TeV, gluons dominate the scattering events.

4 Conclusion

In the beginning part of this work, we gave the derivation of our Generalized Multiplicity Distribution (GMD). We highlighted that GMD has three parameters, namely $\overline{n}$, k, and k'. $\overline{n}$ is the mean multiplicity which can be given directly from experiment. Whereas k and k', being related to the initial number of quarks and gluons respectively, are determined by best-fitting GMD with experimental data. This clearly marks the difference between GMD and Negative Binomial Distribution (NBD) which has only 2 parameters, namely $\overline{n}$ (mean multiplicity) and k (whose interpretation is related to the distribution dispersion in pseudo-rapidity interval). Despite its success however, the phenomenological GMD, as in the case of NBD, is not yet directly derivable from first-principle QCD.

After investigating through all the e^+e^- multiplicity distribution data, we concluded that a single GMD still gives a reasonably good fit for a wide range of data from $\sqrt{s}$ as low as 14 GeV to 189 GeV, even though a slight "shoulder" starts developing at 133 GeV. Whereas, a superposition of 2 GMDs is needed to describe $p\overline{p}$ and pp data accurately, where one GMD describes the soft component, while the other describes the semihard component of the scattering events. It is tempting to link the "shoulder" structure in the KNO distribution plots to the "ear"-like structure of the Lee-Yang circles: the "ear" is converging as the "shoulder" is developing. The development of the "shoulder" is due to the semihard component which becomes more significant as $\sqrt{s}$ increases. Hence, we would expect that the transition from soft to semihard component is carried by the transition from quark-dominating scattering to gluon-dominating scattering of which the underlying mechanism still eludes us.

Extending our prediction to 14 TeV, we expect that the gluon-dominating scattering to dominate as well as such high energy range. The "shoulder" in the distribution plot as well as the "ear"-like structure in the Lee-Yang plot will be much more pronounced, and it can be an obvious hint to confirm our prediction. As such, we are eagerly waiting for

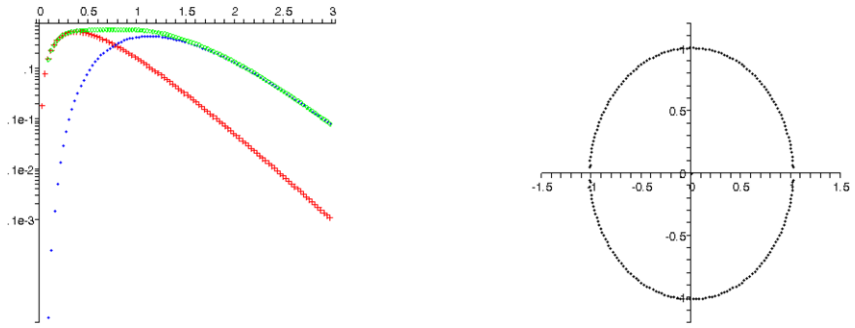

(a) $\sqrt{s} = 14$ TeV, $k'_{semihard} = 6$, $n = 6$ to 200

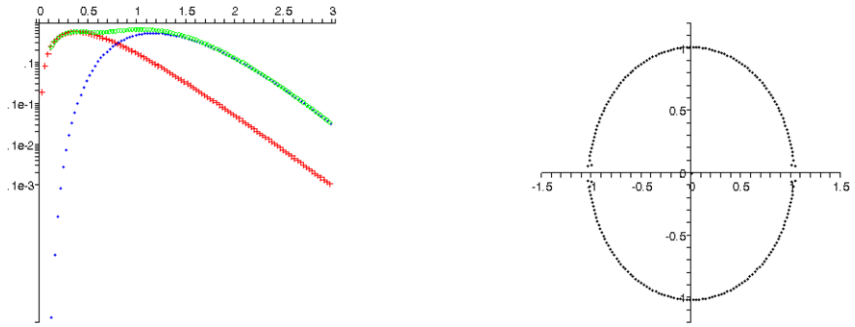

(b) $\sqrt{s} = 14$ TeV, $k'_{semihard} = 8$, $n = 8$ to 200

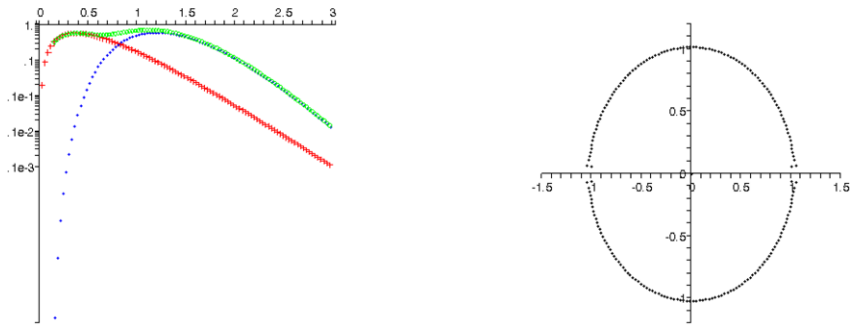

(c) $\sqrt{s} = 14$ TeV, $k'_{semihard} = 10$, $n = 10$ to 200

Fig. 5 KNO and GMD Lee-Yang zeros plot for $\sqrt{s} = 14$ TeV. The "shoulder" structure is signified by the increasing k'_{semihard} value

the real LHC's pp scattering data at 14 TeV to check the link between the "shoulder structure" and Lee-Yang circles.

Acknowledgement This work is supported by NUS academic research grant No. WBS: R-144-000-178-112.

References

1. A. Giovannini, R. Ugoccioni, J. Phys. Conf. Ser. **5**, 190 (2005)
2. R. Ugoccioni, A. Giovannini, J. Phys. Conf. Ser. **5**, 199 (2005)
3. A. Giovannini, Nucl. Phys. B **161**, 429 (1979)
4. R. Ugoccioni, A. Giovannini, Nucl. Phys. B (Proc. Suppl.) **71**, 211 (1999)
5. R.E. Ansorge, Z. Phys. C **43**, 357 (1989)
6. P. Abreu, Z. Phys. C **50**, 185 (1991)
7. C.K. Chew, D. Kiang, H. Zhou, Phys. Lett. B **186**(3), 411 (1987)
8. A.K. Wroblewski, in *Proceedings of the 25th International Conference on High Energy Physics*, vol. 1 (World Scientific, Singapore, 1991), p. 125
9. A.H. Chan, C.K. Chew, Z. Phys. C **55**, 503 (1992)
10. A. Capella, I.M. Dremin, V.A. Nechitailo, J. Tran Thanh Van, Z. Phys. C **75**, 89 (1997)
11. C. N Yang, T.D. Lee, Phys. Rev. **87**(3), 404 (1952)
12. C. N Yang, T.D. Lee, Phys. Rev. **87**(3), 410 (1952)
13. T.C. Brooks, K.L. Kowalski, C.C. Taylor, Phys. Rev. D **56**(9), 5857 (1997)
14. M. Brambilla, A. Giovannini, R. Ugoccioni, J. Phys. G: Nucl. Part. Phys. **32**, 859 (2006)
15. R.C. Hwa, C.S. Lam, Phys. Lett. B **173**, 346 (1986)
16. TASSO Collaboration, Z. Phys. C **22**, 307 (1984)
17. AMY Collaboration, Phys. Rev. D **42**(3), 737 (1990)

18. DELPHI Collaboration, Z. Phys. C **50**, 185 (1991)
19. OPAL Collaboration, Z. Phys. C **72**, 191 (1996)
20. OPAL Collaboration, Z. Phys. C **75**, 193 (1997)
21. OPAL Collaboration, Eur. Phys. J. C **16**, 185 (2000)
22. A. Dewanto, A.H. Chan, C.H. Oh, Int. J. Mod. Phys. E **16**, 3295 (2007)
23. UA5 Collaboration, Z. Phys. C **43**, 357 (1989)
24. UA5 Collaboration, Phys. Rep. **154**, 247 (1987)
25. A. Giovannini, R. Ugoccioni, Nucl. Phys. B (Proc. Suppl.) **64**, 68 (1998)